INTERNATIONAL JOURNAL OF
ENERGY AND ENVIRONMENT

Volume 4, Issue 4, 2013 pp.549-560

Journal homepage: www.IJEE.IEEFoundation.org

Optimization of power generation from shrouded wind turbines

Tudor Foote, Ramesh Agarwal

Department of Mechanical Engineering and Materials Science, Washington University in St. Louis, USA.

Abstract
In past several years, several studies have shown that the shrouded wind turbines can generate greater power compared to bare turbines. The objective of this study is to determine the potential of shrouded wind turbines for increased power generation by conducting numerical simulations. An analytical/computational study is performed by employing the well-known commercial Computational Fluid Dynamics (CFD) software FLUENT. An actuator disc model is used to model the turbine. The incompressible Navier-Stokes equations and a two equation realizable k – ε model are employed in the calculations. The power coefficient Cp and generated power are calculated for a large number of cases for horizontal axis wind turbines (HAWT) of various diameters and wind speeds for both bare and shrouded turbines. The design of the shroud is optimized by employing a single objective genetic algorithm; the objective being the maximization of the power coefficient Cp. It was found that the shroud indeed increases the Cp beyond the Betz's limit significantly and as a result the generated power; this effect is consistent with that found in the recent literature that the shrouded wind-turbines can generate greater power than the bare turbines. The optimized shape of the shroud or diffuser further increases the generated power and Cp.
Copyright © 2013 International Energy and Environment Foundation - All rights reserved.

Keywords: Shrouded wind turbines; CFD simulations; Shroud optimization; Genetic algorithm; Actuator disk model; Betz iimit.

1. Introduction

In past several years, several studies have shown that the shrouded wind turbines can generate greater power compared to bare turbines. An analytical/computational study is performed to evaluate this potential by employing the well-known commercial Computational Fluid Dynamics (CFD) software FLUENT [1]. An actuator disc model is used to model the turbine [2-5]. First, the mathematical model (actuator disc model), using FLUENT, is validated by computing the pressure coefficient (Cp) for a bare turbine; Cp value close to Betz's limit (~0.59), Manwell et. al. [3] is obtained. In the validation, the flow is assumed to be inviscid, incompressible and irrotational (potential flow). After the validation, calculations are performed for a large number of cases for horizontal axis wind turbines (HAWT) of various diameters and wind speeds for both bare and shrouded turbines. The incompressible Reynolds - Averaged Navier-Stokes (RANS) equations with a two equation realizable k–ε model are employed in the calculations. The design of the shroud is optimized by employing a single objective genetic algorithm [6, 7]; the objective being the maximization of the power coefficient Cp. It was found that the shroud indeed increases the Cp beyond the Betz's limit significantly and as a result the generated power; this

effect is consistent with that found in the recent literature that the shrouded wind-turbines can generate greater power than the bare turbines [8, 9]. The optimized shape of the shroud or diffuser further increases the generated power and Cp.

2. Technical approach

The performance of a wind turbine inside a shroud is modeled by creating an actuator disc model in the CFD commercial solver FLUENT. The schematic of the geometry of the configuration used in the computations is shown in Figure 1. Turbine radius (R_t), wind speed (V_o), shroud exit area to turbine area ratio (R_e/R_t), and shroud exit length ($L2_{max}$) are the key parameters that were varied to determine Cp and generated power for shrouded wind turbines. The shroud shape was optimized using a genetic algorithm (GA). Thirteen optimization cases were computed by varying various parameters which are summarized in Table 1.

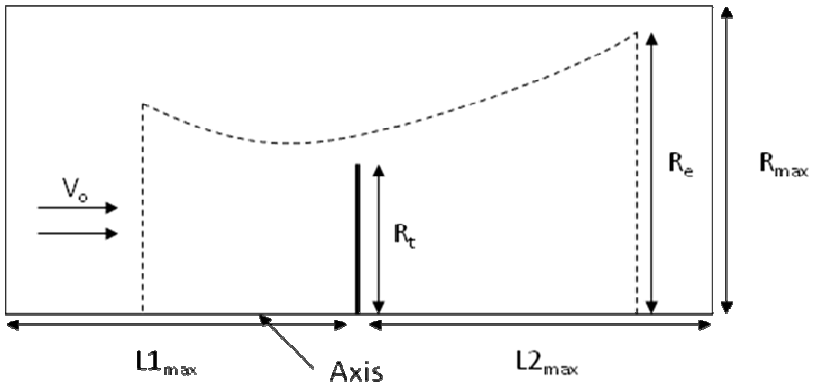

Figure 1. Schematic of axisymmetric HAWT actuator disk model and shroud parameters

Table 1. Parameters of thirteen computed cases

Case #	R_t (ft)				V_o (m/s)		R_e/R_t			$L2_{max}/R_t$		
	1.5	5.0	8.0	10.0	5.71	7.0	2.0	2.56	3.0	1.0	2.0	3.0
1a		X			X			X		X		
1b		X				X		X		X		
1c		X			X		X				X	
1d		X			X				X			X
1e		X			X				X		X	
1f		X			X				X	X		
1g		X			X		X			X		
2a			X		X			X		X		
2b			X			X		X		X		
3a	X				X			X		X		
3b	X					X		X		X		
4a				X	X		X				X	
4b				X		X	X				X	

The mesh inside the geometry of Figure 1 was generated using the ANSYS software "GAMBIT" [10]. The flow field simulations were performed using the CFD solver FLUENT [1]. The incompressible Reynolds - Averaged Navier-Stokes (RANS) equations with a two equation realizable k – ε model were employed in the calculations. A first-order upwind scheme with adaptive structured mesh was used in the calculations. Successively refined meshes were used to determine the best mesh to obtain mesh-free accurate solution. Each of the turbine case in Table 1 is called an individual. GAMBIT and FLUENT are used to determine Cp for each individual. For each case in Table 1, a number of individuals (with different shroud shapes) were generated and their Cp was calculated. The genetic algorithm (GA) was then employed to determine the best shroud shape to obtain the maximum Cp (the fitness or objective function value) for that case in Table 1. The details of the genetic algorithm are given in section 3. Figure 2 shows the schematic of the computational process using the GA based optimizer with FLUENT.

 ©2013 International Energy & Environment Foundation. All rights reserved.

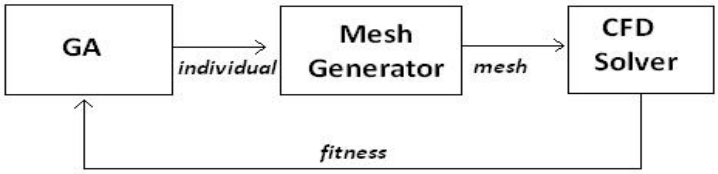

Figure 2. Schematic of the computational process using the GA based optimizer with FLUENT

3. Brief description of genetic algorithm

In this section, we briefly describe the genetic algorithm (GA) employed in this work. We first discuss the GA optimization technique, followed by the parameterization of the shroud and implementation details of GA.

3.1 Single objective genetic algorithm (SOGA)

Genetic algorithms are a class of stochastic optimization algorithms inspired by the biological evolution. In GA, a set or generation of input vectors, called individuals, is iterated over, successively combining traits (aspects) of the best individuals until a convergence is achieved. In general, GA employs the following steps [6, 7].

1. Initialization: Randomly create N individuals.
2. Evaluation: Evaluate the fitness of each individual.
3. Natural selection: Remove a subset of the individuals. Often the individuals that have the lowest fitness are removed; although culling, the removing of those individuals with similar fitness, is sometimes performed.
4. Reproduction: Pick pairs of individuals to produce an offspring. This is often done by roulette wheel sampling; that is, the probability of selecting some individual h_i for reproduction is given by:

$$P[h_i] = \frac{fitness(h_i)}{\sum_j fitness(h_j)} \tag{1}$$

A *crossover* function is then performed to produce the offspring. Generally, crossover is implemented by choosing a crossover point on each individual and swapping *alleles* – or vector elements – as illustrated in Figure 3.

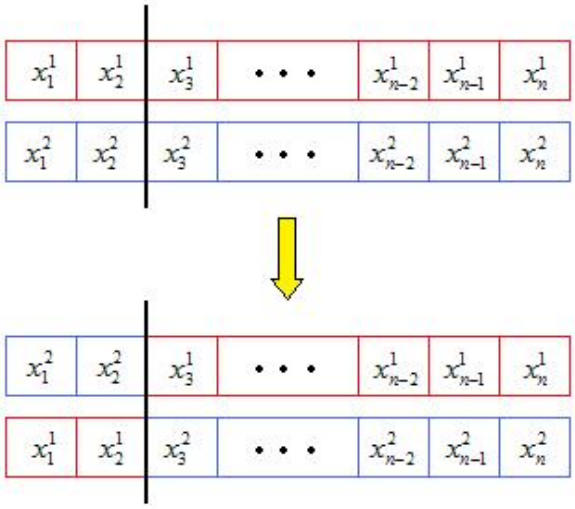

Figure 3. Illustration of the crossover function in GA

5. Mutation: Randomly alter some small percentage of the population.
6. Check for Convergence: If the solution has converged, return the best individual observed. If the solution has not yet converged, label the new generation as the current generation and go to step 2. Convergence is often defined by a certain number of generations or a similarity threshold.

 ©2013 International Energy & Environment Foundation. All rights reserved.

3.2 Shroud parameterization

Each individual shroud shape is represented by a Bezier curve. Pierre Bezier developed the parametric curve in 1962 to have a finite way to describe the complex contours of automobile body shapes. It works by having a series of control points that are related by a parametric equation. The general form of that equation is given below as equation (2) where *n* is the number of control points *P*.

$$B(t) = \sum_{i=0}^{n} \binom{n}{i} (1-t)^{n-i} t^i P_i \tag{2}$$

Seven control points, each with radial and axial coordinates, were used to describe the shroud shapes. The control points for the HAWT shroud were defined such that they were axially ordered with the middle control point within 1 axial foot of the turbine position, and three points on either side. For the shroud shapes generated in this work, the complexity of the curves on either side of the turbine was sufficient to describe the optimized shapes. Limits were set for the maximum dimensions of the control points to simulate cost and practicality requirements, and to prevent the shroud from becoming infinitely large. Figure 4 shows an example curve (for Case 1a in Table 1 above) and its corresponding control points. Note that the control point on the far right reached both the maximum radius of 8 ft. and the maximum distance from the turbine plane of 5 ft., as set by the limits.

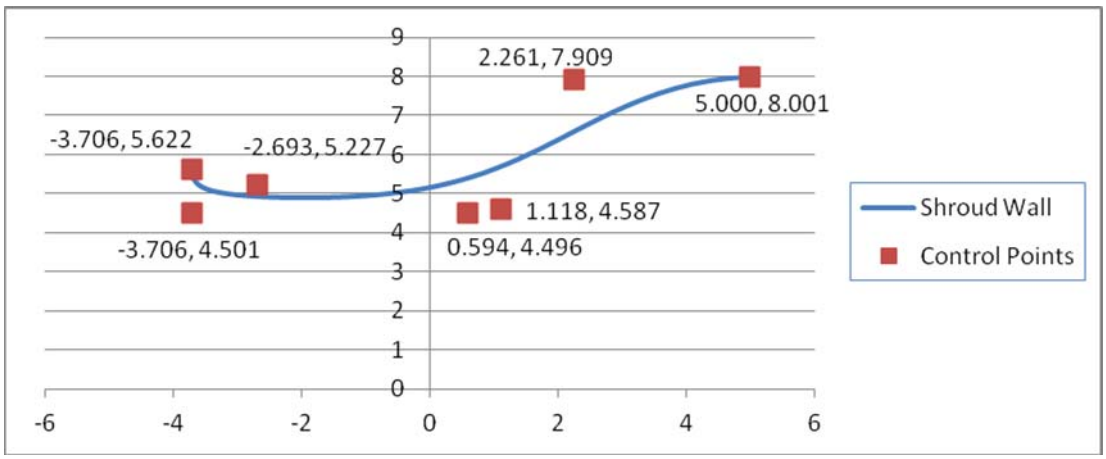

Figure 4. Optimized shroud shape with control points for Case 1a in Table 1

3.3 Evaluation of an individual

For any individual, the GA creates a data file from its control points that contains vertices for all the relevant points of the geometry. The GA then runs a batch file that opens the mesh generator and tells it to run a journal file that takes the geometry data file and creates a mesh. The journal must be robust enough to account for the possible variation in the geometries and still build a usable mesh. Therefore, a fixed number of nodes are defined on the surfaces of the adjustable shape (the shroud wall) and the mesh generator fits a fixed number of quadrilateral cells into the geometry based on those nodes. The cells conform to the geometry even though the diffuser in the computational domain may change in geometry during the GA convergence process. Once the GA detects that the mesh generator has finished, it calls a cleanup batch file to erase unnecessary temporary files, and then calls another batch file that opens the CFD flow solver. This too has a robust journal file that sets the correct parameters and solves the flow on the mesh that was just created. This journal is modified by the GA for each individual before the flow solver runs to ensure it has the correct pressure drop value determined by the actuator disk theory for that individual. Once the flow solver finishes, it records the fluid area-averaged flow velocity through the actuator disk. This is then read by the GA and is used to calculate the fitness of the shroud shape. The GA also imposes a penalty function for any control point that moves outside its intended domain by reducing its fitness by a factor of the distance out of bounds. If there is an error such that the flow solver does not return a value, for example if the mesh is physically impossible or the solver diverges and returns an unreasonable value, the fitness of the individual is set to -1 so that natural selection will remove it from the next generation, but it still contributes to the breeding process explained below.

 ©2013 International Energy & Environment Foundation. All rights reserved.

3.4 Advancing the generation with crossover and mutation

In the implementation of the GA for shroud optimization, a generation size of 20 individuals is used with a natural selection rate of 50% with no culling tolerance; that is, no attempt is made to remove similar shrouds. Once the fitness values of all the individuals in a generation are determined, the worse 50% of each generation are replaced through an extrapolation-based crossover scheme. Reproduction is initiated by randomly selecting two individuals in the generation. The offspring individual is obtained by moving the components of each control point according to equation (3) below. Each new control point is set beyond the more fit parent's control point value from the lesser fit parent's control point value. The distance it is moved beyond is a random fraction of the distance between the parents' control points.

$$crossover(x_1, x_2) = rand(0,1) \cdot (x_1 - x_2) + x_2 \tag{3}$$

Once the new generation of 20 shroud shapes is created, the mutation procedure occurs. A random number generator uses the mutation rate to decide how many of the 20 individuals to remove and replace them with new randomly generated individuals. Mutation allows for the possibility of rapid changes and advancement. It also guards against becoming stuck in a relative maximum of fitness and missing the true maximal arrangement.

Each configuration was run in the GA for 350 generations, as this was determined to be sufficient for reasonable convergence without excessive computing time. The number of control points was a large factor in determining the necessary number of generations. The crossover function moves all the control points, so they must be simultaneously optimized. The random guesses made in the first generation and by mutation can accelerate the process significantly. The best way to make the process more rapid is to have small domains for each control point so that the random individuals will be close to the optimum. This however runs the risk of placing the domains in the wrong positions and not obtaining the optimum individual. The control points of the final individual must be checked to see if they are on a boundary condition as this may indicate its optimum position is beyond the boundary.

3.5 Solution convergence

As mentioned previously, if the solution has converged, return the best individual observed and that is the desired shape. If the solution has not converged, label the new generation as the current generation and go to 3.3. Convergence is often defined by a certain number of generations or a similarity threshold.

4. Results and discussion

In this section, we first describe the optimized shroud shape and solution obtained for case 1(a) of Table 1. Following the procedure outlined in Figure 2, first an adaptive structured mesh was generated using GAMBIT. The mesh inside the optimal shroud shape with the actuator disk is shown in Figure 5. Note that only half of the domain about the centerline of the diffuser is shown because of symmetry. Figure 6 shows the total pressure distribution upstream and downstream of the actuator disk; it clearly shows the discontinuity in the total pressure across the actuator disk as expected.

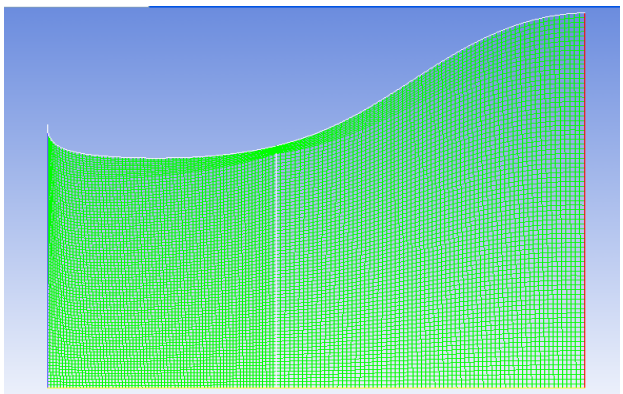

Figure 5. Mesh inside the shroud for case 1(a)

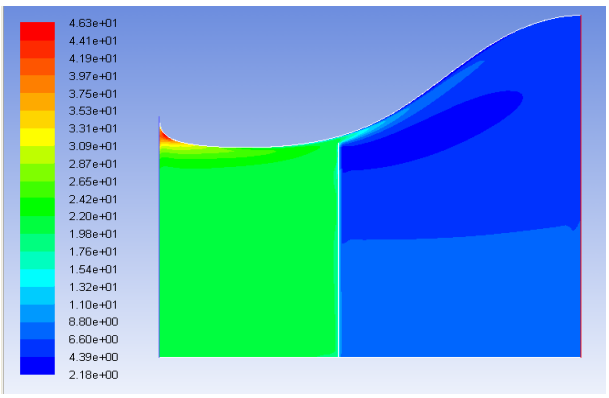

Figure 6. Total pressure inside the shroud for case 1(a)

 ©2013 International Energy & Environment Foundation. All rights reserved.

Figures 7 and 8 respectively show the static pressure distribution and the velocity magnitude contours inside the shroud for case 1(a) of Table 1.

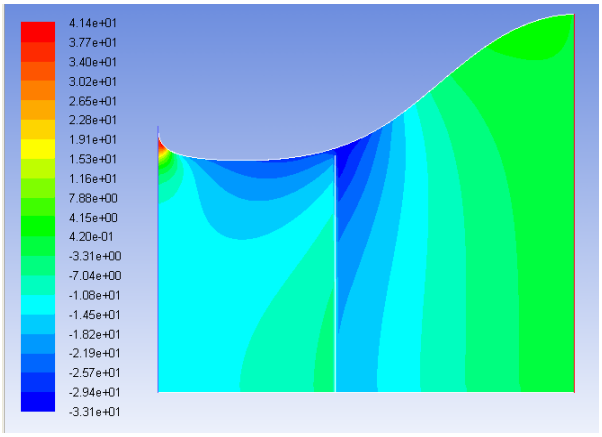

Figure 7. Static pressure contours inside the shroud for case 1(a)

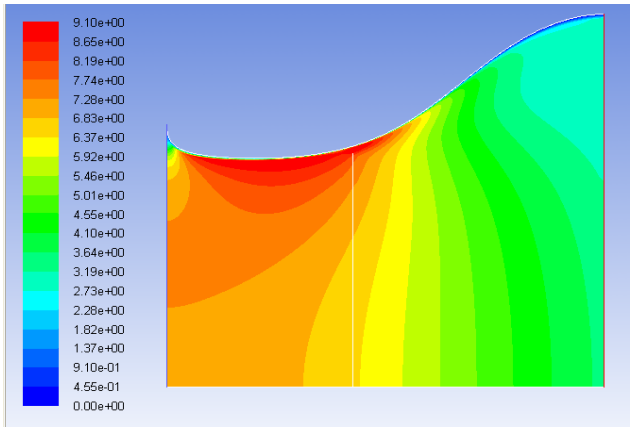

Figure 8. Velocity magnitude contours inside the shroud for case 1(a)

Figures 9 and 10 respectively show the variation in velocity and the change in static pressure distribution along the axis of the shroud for case 1(a) of Table 1. Figure 11 shows the change in the total pressure along the axis of the shroud. Figures 10 and 11 clearly show the jump in both the static pressure and total pressure across the actuator disk.

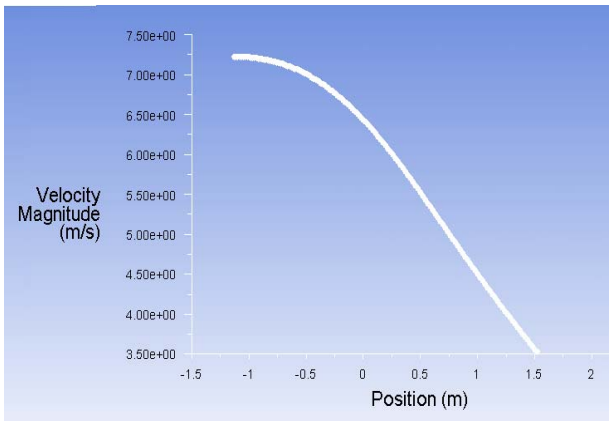

Figure 9. Velocity variation along the centerline of the shroud for case 1(a)

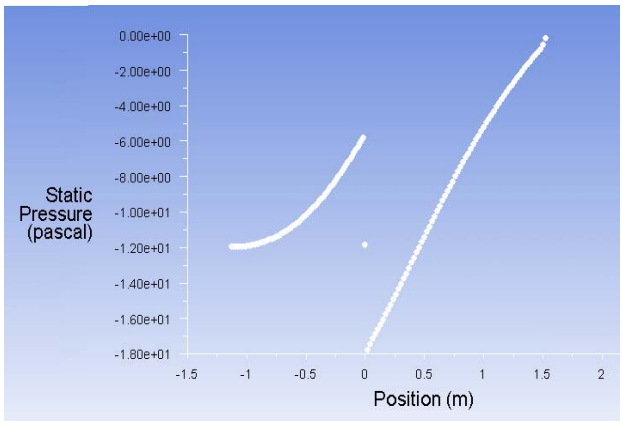

Figure 10. Static pressure variation along the axis of the shroud for case 1(a)

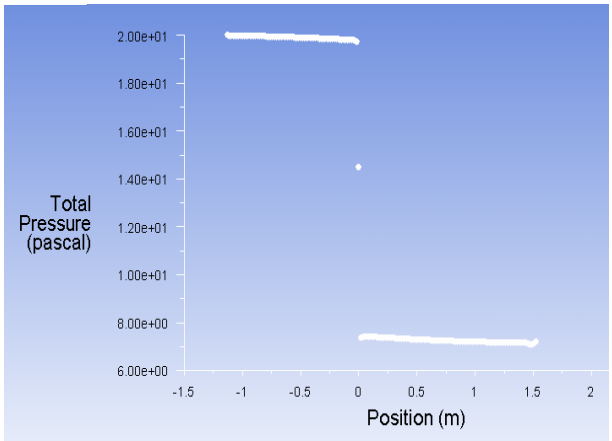

Figure 11. Total pressure variation along the axis of the shroud for case 1(a)

 ©2013 International Energy & Environment Foundation. All rights reserved.

Optimal shapes for all the thirteen cases shown in Table 1 were obtained using the procedure outlined in Figure 2. Flow field results similar to those shown in Figures 5-11 were obtained.
Figure 12 shows the optimized shroud shapes obtained for maximum Cp for the thirteen cases whose parameters are given in Table 1. Table 2 gives the power production data and Cp for the thirteen optimized shroud cases.

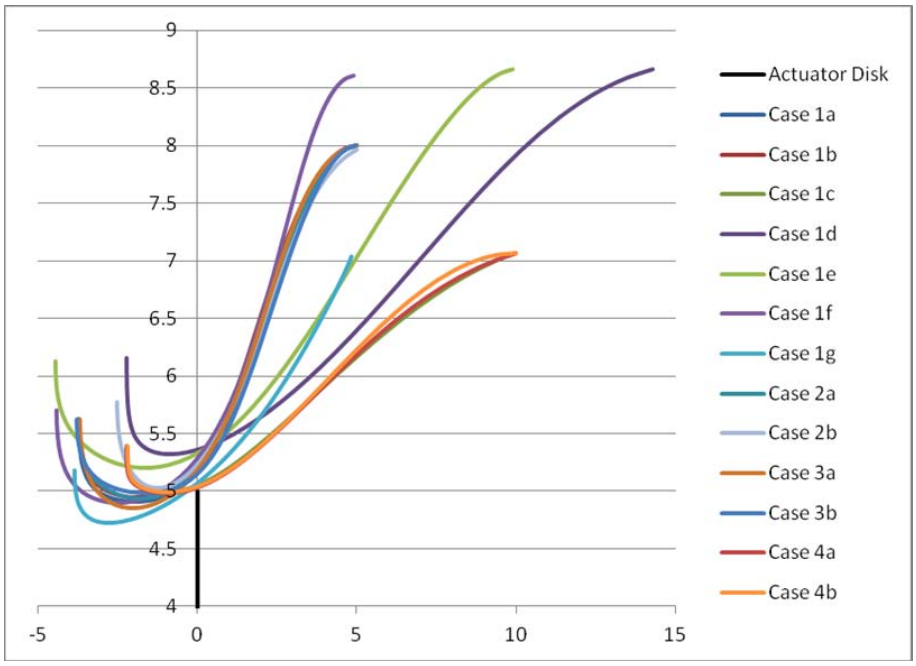

Figure 12. Thirteen optimized diffuser shapes for thirteen cases in Table 1 for a 5 ft radius turbine (shown as an actuator disk)

Table 2. Power production and power coefficient Cp for thirteen cases of Table 1

Case	Power (W)	Cp
1a	717	0.86
1b	1294	0.84
1c	642	0.77
1d	889	1.07
1e	861	1.03
1f	755	0.91
1g	582	0.70
2a	1849	0.87
2b	3321	0.85
3a	65	0.87
3b	117	0.85
4a	2540	0.76
4b	4637	0.76

Next, we examine the effect of various geometric and operation parameters on power production and Cp.

4.1 Effect of turbine radius on Cp

The scale of the turbine over the range of radii computed does not seem to have a discernible effect on Cp. Two sets of identical calculations at two wind speeds show little difference in performance outside the margin of error in the simulations as can be seen in Figure 13. Figure 14 shows the shroud shapes of these cases and they are quite similar. This is consistent with the fact that viscous effects do not become dominant until the turbine radius becomes much smaller than those analyzed in this work.

 ©2013 International Energy & Environment Foundation. All rights reserved.

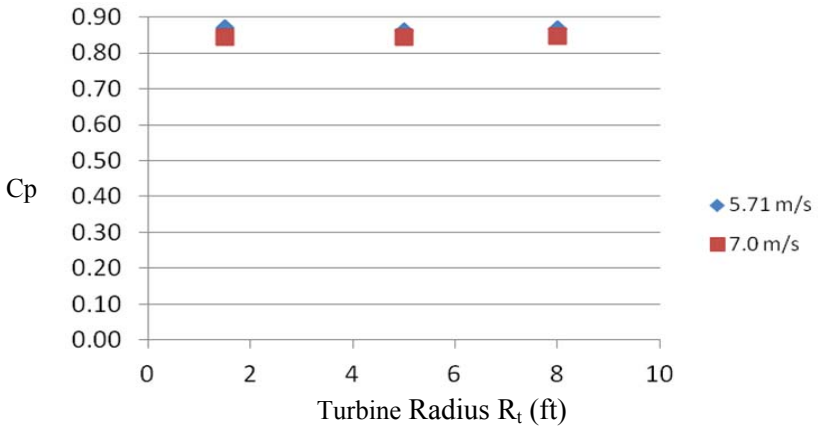

Figure 13. Variation of Cp with turbine radius at two free stream wind velocities (5.71 m/s and 7.0 m/s)

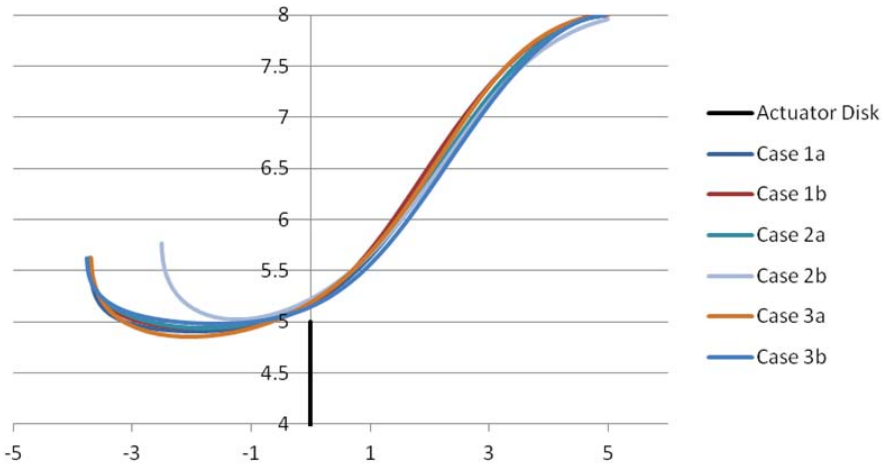

Figure 14. Similar shroud shapes are obtained for six cases of Figure 13 scaled to a turbine radius of 5 ft

4.2 Effect of wind speed on Cp

The effect of wind speed on shroud shape and performance was small but consistent. Figure 13 shows that the higher velocity shrouds were slightly less productive in power generation. Viscous losses due to the higher wind speeds are the most likely cause of this small change in power generation.

4.3 Effect of shroud exit area to turbine area ratio

The ratio of the shroud exit area to the turbine area was the primary factor in determining shroud performance. A strong positive correlation was observed for all cases as shown in Figure 15 below. The larger diffusers caused greater flow velocities at the actuator disk, leading to higher power coefficients Cp.

4.4 Effect of Shroud Exit Length

The length of the diffuser behind the actuator disk, L2, is not a primary factor in determining the performance of a shroud. Figure 16 shows significant variation in Cp at both shorter and larger lengths but does not indicate a clear trend in Cp vs. L2 for the cases considered in this study. However, the three cases, (Case 1d, Case 1e, and Case 1f) where all other factors are held equal except the length L2 indicate a strong trend as seen in Figure 17; Cp increases significantly with L2. The primary driver of this trend is the flow separation near the surface of the diffuser. All three cases have the same exit area which is three times the turbine area. The shorter diffusers create such steep angles that the flow separates and the diffusers become less efficient. The three shroud shapes for cases 1d, 1e and 1f are shown together in Figure 18. Case 1f did not expand to its maximum allowable value of L2, suggesting that it is at an optimum angle.

 ©2013 International Energy & Environment Foundation. All rights reserved.

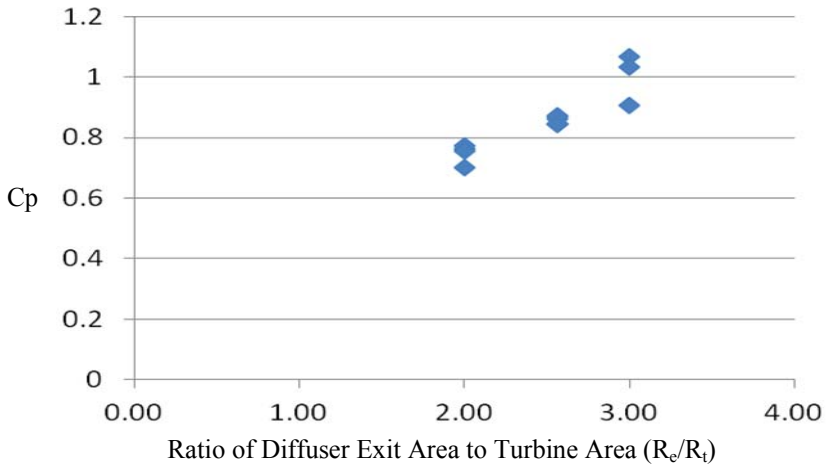

Figure 15. The effect of ratio of the shroud exit area to turbine area ratio on Cp

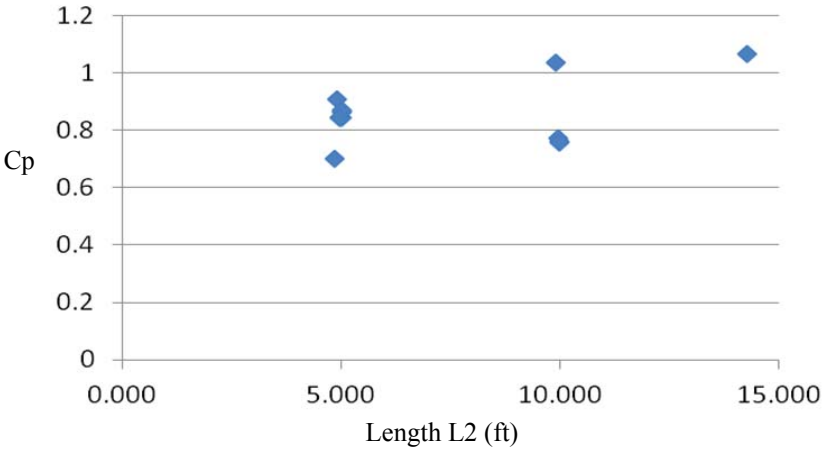

Figure 16. Change in Cp for shrouds of various lengths L2

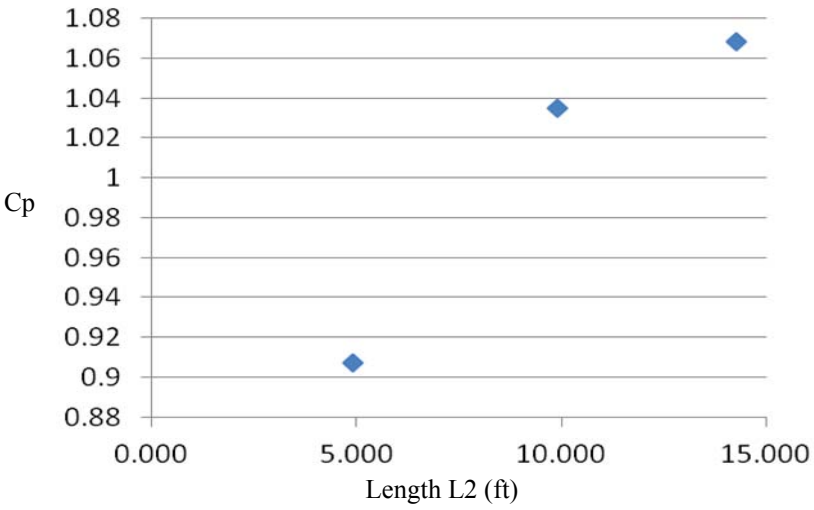

Figure 17. Change in Cp with L2 for cases 1d, 1e, and 1f in Table 1

ISSN 2076-2895 (Print), ISSN 2076-2909 (Online) ©2013 International Energy & Environment Foundation. All rights reserved.

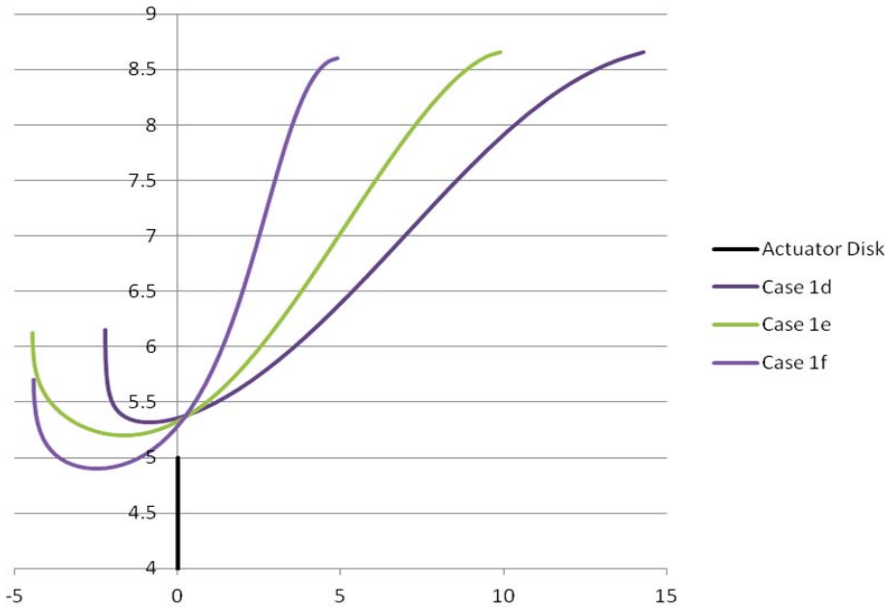

Figure 18. Optimized Shroud shapes for cases 1d, 1e, and 1f

5. Comparison of present results with those of Werle and Presz [9]

Werle and Presz [9] have computed the effect of shroud on HAWT performance; Figure 19 from their paper [9] shows the variation of maximum power coefficient of a shrouded wind turbine to its thrust coefficient. Figure 19 shows the calculations using the inviscid theoretical analysis as well as the CFD analysis including the results for both the ducted and bare wind turbine. Figure 20 shows our CFD calculations for eight optimized shrouds and their comparisons with the results in Figure 19. Our results for optimized shrouds in Figure 20 agree quite well with those of Werle and Presz [9]. They all fall close to the region circled in Figure 19 for ducted wind turbines. This comparison is an affirmation that the Genetic Algorithm and the flow modeling described in this paper are quite accurate.

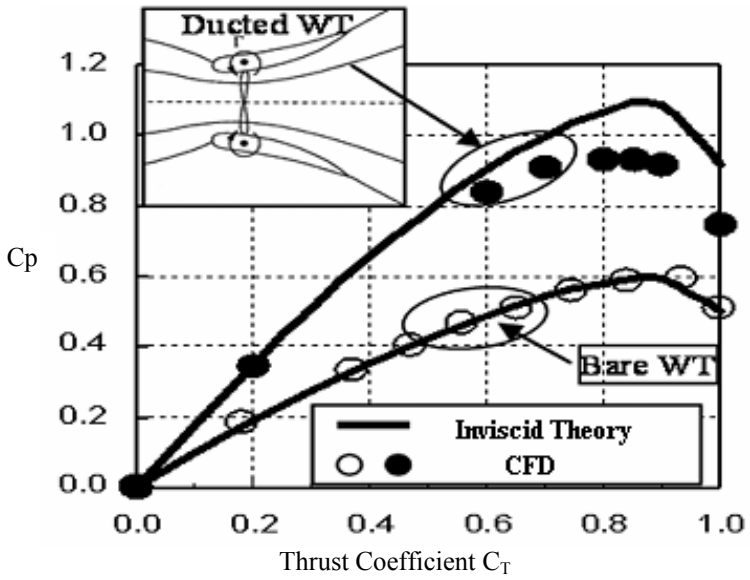

Figure 19. Variation of Cp with C_T for a bare and shrouded wind turbine from Werle and Presz [9]; the solid line is the theoretical calculation using the inviscid theory, the open and dark circles represent the CFD results from References 2 and 9

 ©2013 International Energy & Environment Foundation. All rights reserved.

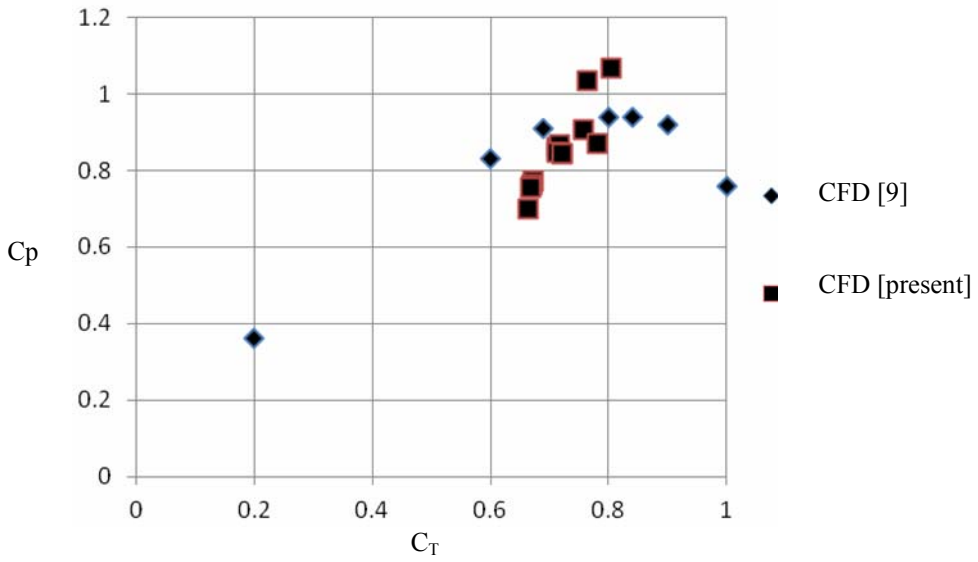

Figure 20. Comparison of Cp vs. C_T results for eight optimized shrouded wind turbines with those of Werle and Presz [9]

Due to the GA finding the optimum pressure coefficient at the actuator disk, the full range of thrust coefficients shown in Figure 20 could not be obtained for the thirteen optimized shrouds computed in this paper. In order to demonstrate the trend shown by the CFD data in Werle and Presz's paper [9] the pressure coefficient was varied in the optimized shroud of Case 2a from 0.05 to 1.5 and resolved for the Cp and C_T. Figure 21 shows the close correlation with the curve in Werle and Presz [9]. Case 2a's maximum Cp occurs at the point using the pressure coefficient calculated by GA. The deviation at high thrust coefficients is due to the tip gap between the turbine and the diffuser present in this work and not in Werle and Presz's work [9]. As the actuator disk exerts more back pressure on the flow, a greater portion of it escapes through the gap resulting in a loss of pressure and power generation.

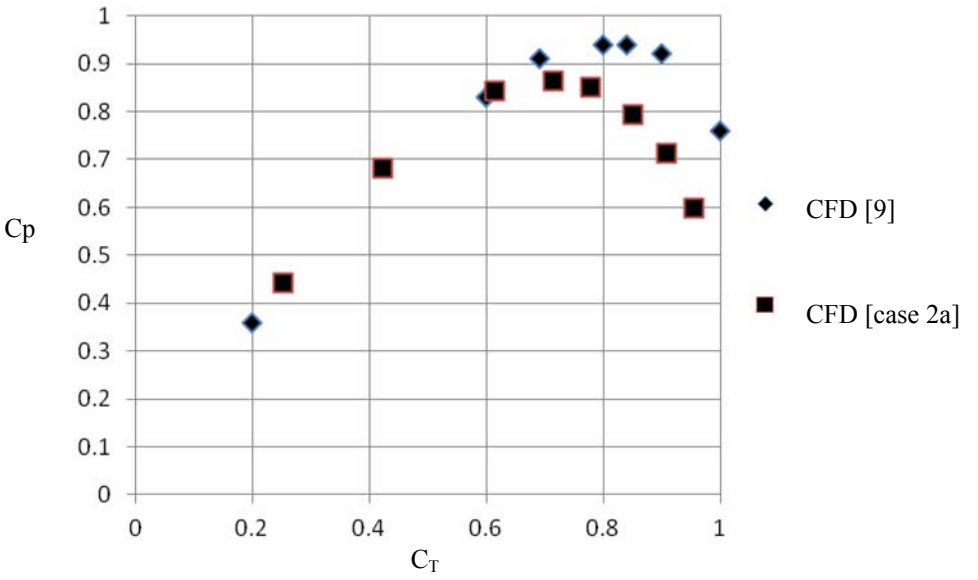

Figure 21. Comparison of Cp vs. C_T for optimized shroud of Case 2a with those of Werle and Presz [9]

6. Conclusions

The results presented in this paper demonstrate that shrouded wind turbine can generate more power and hence have a higher power coefficient than that for the bare turbine which is limited by the Betz's limit. The optimization of the shape of the shroud can further maximize the generated power.

ISSN 2076-2895 (Print), ISSN 2076-2909 (Online) ©2013 International Energy & Environment Foundation. All rights reserved.

References

[1] FLUENT 6.3, 2007. Flow Modeling Software, Ansys Inc.
[2] Mikkelsen R. Actuator Disc Methods Applied to Wind Turbines. PhD Thesis, Technical University of Denmark, Copenhagen, June 2003.
[3] Manwell J.F., McGowan J.G., and Rogers A.L. Wind Energy Explained. John Wiley, 2nd edition 2009.
[4] Hansen M.O.L. Aerodynamics of Wind Turbines. Earthscan, Sterling, VA, 2000.
[5] Burton T., Sharpe D., Jenkins N., and Bossanyi E. Wind Energy Hand Book. John Wiley.
[6] Goldberg D.E., 1989. Genetic Algorithms in Search, Optimization & Machine Learning. Addison-Wesley, 2001.
[7] Morgan B. Gairfoils: Finding High-Lift Joukowski Airfoils with a Genetic Algorithm. Dept. of Mechanical Engineering & Materials Science Technical Report, Washington University in St. Louis, 2007.
[8] Hansen M.O.L., Sorenson, N.N., and Flay R.G.J. Effect of Placing a Diffuser around a Wind Turbine. Wind Engineering, 2000, Vol. 3, No. 4, pp. 207-213.
[9] Werle M.J. and Presz Jr. W.M. Shroud and Ejector Augmenters for Subsonic Propulsion. AIAA J. of Propulsion and Power, 2009, Vol. 25, No. 1, pp. 228-236.
[10] GAMBIT 6.2. Geometry and Mesh Generation Preprocessor, Ansys Inc, 2007.

Tudor Foote graduated with a M.S in Mechanical Engineering in December 2011 from the Department of Mechanical Engineering & Materials Science at Washington University in St Louis. He received B.S. in Mechanical Engineering also from Washington University. Tudor's research focuses on wind energy and aerodynamics. He is currently working on shape optimizations for shrouds for small horizontal-axis wind turbines (HAWT) using CFD method and genetic algorithm
Email address: tffoote@gmail.com

Ramesh K. Agarwal received the Ph.D degree in aeronautical sciences from Stanford University, Palo Alto, CA, USA in 1975. His research interests are in the theory and applications of computational fluid dynamics to study the fluid flow problems in aerospace and renewable energy systems. He is currently the William Palm Professor of Engineering in department of Mechanical Engineering and Materials Science at Washington University in St. Louis, MO, USA. He is a Fellow of ASME, AIAA, IEEE, and SAE.
Email address: rka@wustl.edu

 ©2013 International Energy & Environment Foundation. All rights reserved.